

# Senior Design Summary

Jonathon McBride, Alexandra Nilles, Keith Schumacher  
Advisor: Dr. Mark Lusk

May 12, 2014

# 1 Introduction

## 1.1 Overview

The aim of this project was to use the recently developed hierarchical equations of motion (HEOM) [1] to model coherent exciton transport dynamics within various small molecular systems. We investigated inter-molecular exciton transport, and found molecular characteristics that favor coherent (wave-like) transport over ballistic (particle-like) transport. Our research into organic molecules was inspired by observations of photosynthetic light-harvesting complexes. The Fenna-Matthews-Olson (FMO) complex uses interactions between excitons and the vibrational modes of the system to transport energy in a partially-coherent manner [2]. Dr. Mark Lusk, the advisor of this project, has an active research interest in exciton transport - the design of next-generation solar cells which utilize quantum effects could revolutionize energy transport.

The last few years have brought important theoretical developments in our ability to model coherent transport. For decades, the Redfield equation was used to model open quantum systems, but this model is limited. For example, the Born approximation in the Redfield model assumes weak interactions between a molecular system and its environment. As a result, the Redfield model cannot account for the relatively strong system-environment interactions in room-temperature situations [1] such as actual solar cells.

Additionally, the Markov approximation utilized in the Redfield model assumes that the system phonons are always in an equilibrium state [3]. However, if the system absorbs a photon (electronic excitation), the vibrational energy states of the system can also become excited for a brief time due to exciton-phonon coupling [4]. The difference in energy between the equilibrium and excited phonons is known as the reorganization energy. While the Redfield model assumes limited electron-phonon interaction, the magnitude of the reorganization energy is now thought to influence exciton behavior. The Redfield model is useful in some contexts, but for short-lived coherence analysis, a new model is needed.

The hierarchical equations of motion (HEOM) were developed by Ishizaki and Fleming [1][5] in 2009. These equations do not assume weak electron-phonon interaction and are not based on any perturbation arguments. Thus the approach has the potential to be a much more accurate model for room-temperature exciton transport. The HEOM have been numerically implemented on graphics processing units (GPUs) by Dr. Christoph Kreisbeck [6], and it was this implementation that was used for our research. We used the HEOM to investigate the relationship between the physical structure of systems and the behavior of excitons in those systems. Specifically, we analyzed the spectral density, which is the functional relationship between phonon modes and the magnitude of the electron-phonon coupling [6]. Using the spectral density and other physical characteristics of systems, we investigated which molecular characteristics encourage coherent transport. We have identified several desirable characteristics for highly-coherent systems, and analyzed several promising molecular geometries.

## 1.2 Systems of Interest

We used the HEOM to model exciton transport in two-site molecular systems. Each site of the system consists of a single molecule, and the two sites are linked together by a molecular bridge.

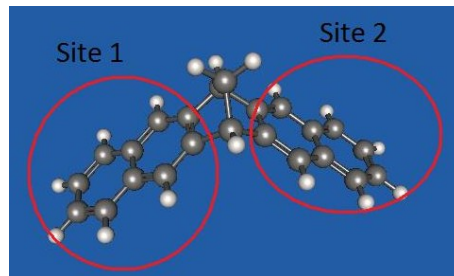


Figure 1: Example of a 2-Site System

The sites of our studied systems are naphthalene molecules, which are two Benzene molecules bonded together to form a dimer chain.

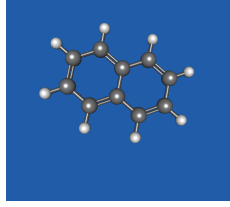


Figure 2: Naphthalene: Molecular Site of Studied Systems

The naphthalene sites are bridged together by poly-norbornene bridges to create the complete systems of study: DN2, DN4, and DN6.

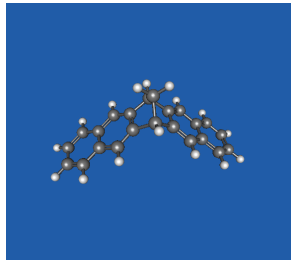


Figure 3: DN2

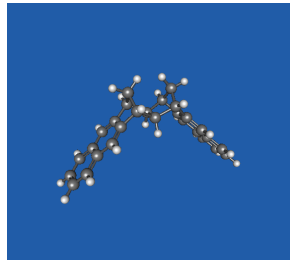


Figure 4: DN4

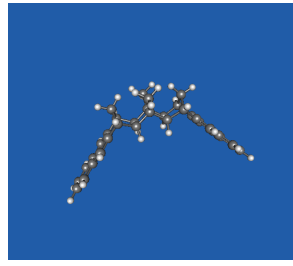


Figure 5: DN6

### 1.3 Coherence Analysis

Consider a situation where one site absorbs a photon, and creates an exciton (an electron-hole pair). The HEOM models the exciton dynamics as a time dependent density matrix. The diagonal elements of the matrix represent the physically measurable exciton populations at each site. Coherence between sites corresponds to off-diagonal elements of the matrix. A totally decoherent system would have no off-diagonal terms, while complete coherence would mean non-zero off-diagonal elements that do not decay with time. The decay of coherence is the process of decoherence. This involves the system tending toward certain pointer states. Some example states are: a spatially localized exciton either stuck at one site or oscillating between the two, or a dissipated and stationary exciton. A completely decohered exciton is spatially localized and undergoing particle-like motion. A completely coherent exciton spreads like a wave. Partially coherent transport means the exciton is both "jumping" and "spreading" in a dynamic way.

Exciton decoherence is unavoidable when an exciton couples with, and dissipates energy into, a molecule and its environment. Any long-lived coherences in the exciton's state will be accompanied by the partially coherent transport regime. So, in order to optimize a molecular system for exciton transport, the coherence lifetime is a useful metric. It is for this purpose that an analysis of of exciton coherence is carried out.

## 2 HEOM Theory and Derivation

The Hamiltonian for the system is given by  $\mathcal{H} = \mathcal{H}_{ex} + \mathcal{H}_{phon} + \mathcal{H}_{ex-ph} + \mathcal{H}_{reorg}$ . Here,  $\mathcal{H}_{ex}$  and  $\mathcal{H}_{phon}$  account for exciton and phonon degrees of freedom.  $\mathcal{H}_{ex-ph}$  and  $\mathcal{H}_{reorg}$  are responsible for the partially coherent dynamics that are of interest. It is valuable to compare the working Hamiltonian to the Hamiltonians used in the two limiting cases. Forster theory is most accurate in the ballistic regime. It achieves this by assuming weak electronic coupling between sites. This corresponds to the intersite term in  $\mathcal{H}_{ex}$  being relatively small [7]. An alternative model is the Redfield equation, which approximates the coherent regime. As stated in the introduction, it achieves this by assuming the phonon modes are always in equilibrium. This corresponds to their being no reorganization term in the Hamiltonian [7].

Focusing on the part of the Hamiltonian that represents coupling between exciton and vibrational degrees of freedom, Ishizaki and Fleming defined:

$$\begin{aligned}\mathcal{H}_{ex-ph} &= \sum_{m=1}^N V_m B_m \\ V_m &= a_m^\dagger a_m \\ B_m &= \sum_{\xi} \hbar \omega_{\xi,m} d_{\xi,m} (b_{\xi,m}^\dagger + b_{\xi,m})\end{aligned}$$

- $a_m^\dagger, a_m$  are creation and anihilation operators of electronic excitations at site m
- $b_{\xi,m}^\dagger, b_{\xi,m}$  are creation and anihilation operators of phonon mode  $\xi$  at site m
- $d_{\xi,m}$  are non-dimensional modal displacement describing how involved each mode is in relaxation process

The goal of HEOM is to model the time evolution of the reduced density operator,  $\rho(t)$ . Note,  $\tilde{A}$  is the interaction picture version of  $A$ . The derivation starts with the Liouville equation,

$$\frac{d}{dt} \tilde{R}(t) = \frac{-i}{\hbar} [\tilde{H}_{ex-ph}, \tilde{R}(t)] = \frac{-i}{\hbar} \tilde{\mathcal{L}}(t) \tilde{\mathcal{R}}(t)$$

and the reduced density operator, reducing the exciton-phonon system to focus on exciton dynamics, is given by

$$\rho(t) = Tr_{photon} R(t)$$

Integrating the Liouville equation yields  $\tilde{\rho}(t) = \tilde{U}(t)\tilde{\rho}(0)$  where the interaction picture propagator is given by

$$\tilde{U}(t) = \langle T_+ \exp(\frac{-i}{\hbar} \int_0^t ds \tilde{\mathcal{L}}(s)) \rangle$$

Here,  $\langle \dots \rangle$  denotes the bath expectation value and  $T_+$  denotes the chronological time operator [6].

Assuming a Gaussian distribution for harmonic vibrations, the bath expectation value can be reduced to two-time correlation functions. This is expressed as:

$$C_m(t) = \langle \tilde{B}_m(\tau) \tilde{B}_m(0) \rangle$$

Assuming phonon modes are uncorrelated between sites, the time evolution operator can be written as

$$\tilde{U}(t) = T_+ \prod_m \exp(\int_0^t ds \tilde{W}_m(s))$$

where

$$\tilde{W}_m(t) = -\frac{1}{\hbar^2} \int_0^t ds \tilde{V}_m^x [S_m(t-s) \tilde{V}(s)^x - i \frac{\hbar}{2} \chi_m(t-s) \tilde{V}_m(s)^o]$$

- $S_m(t) = Re C_m(t)$
- $\chi_m(t) = \frac{-2}{\hbar} Im C_m(t)$

$S_m(t)$  is the symmetrized correlation function.  $\chi_m(t)$  is the response function. Both functions follow from an application of the fluctuation-dissipation theorem (FDT) to the phonon system. FDT describes the dissipation of energy from thermal fluctuations at thermal equilibrium. A classical example of FDT is the derivation of the diffusion constant in terms of a velocity autocorrelation of a brownian particle undergoing motion in a viscous medium.

Finally, the Hierarchical Equations of Motion are formulated. The auxillary operators are given by

$$\tilde{\sigma}^{n_1, \dots, n_N}(t) = T_+ \prod_{m=0}^N (\int_0^t ds e^{-v(t-s)} \tilde{\theta}_m(s))^{n_m} \exp(\int_0^t ds \tilde{W}_m(s))$$

and the time evolution of the reduced density matrix is given by:

$$\frac{\partial}{\partial t} \rho(t) = -\frac{i}{\hbar} \mathcal{L}_e \rho(t) + \sum_m \frac{i}{\hbar} V_m^x \sigma^{(0, \dots, n_m=1, \dots, 0)}(t)$$

Where  $\mathcal{L}_e$  is the liouvillian for the electronic hamiltonian,  $\sigma^{(0, \dots, n_m=1, \dots, 0)}(t)$  are operators for the fluctuations of electronic energy, and dissipation of reorganization energy. Note, the time evolution of  $\sigma(t)$  depends on higher "orders" of  $\sigma(t)$ . The exciton dynamics can now be calculated.

## 3 Parameter Analysis

### 3.1 Overview

In the derivation of the Hierarchical Equations of Motion (HEOM), we need to describe the nature of the coupling between the excitons and the phonon modes of the molecule. We model this coupling using a Drude-Lorentz spectral density:

$$\mathcal{J}(\omega) = \frac{2\lambda\gamma\omega}{(\omega - \omega_0)^2 + \gamma^2} \quad (1)$$

Where:

- $\omega$  refers an arbitrary vibrational frequency of the system.
- $\lambda$  is the reorganization energy of the system, or the energy dissipated after a site is electronically excited (which causes a corresponding vibrational excitation) and the vibrational components of the system reach equilibrium. Has units of energy ( $\hbar\omega$ ), and is directly proportional to the “height” of the Drude-Lorentz peak [7].
- $\gamma$  has units of frequency and is proportional to the “width” of the Drude-Lorentz peak. Physically,  $\gamma$  can be interpreted as an energy. A smaller  $\gamma$  corresponds to a narrower peak, or a smaller range of energetic coupling between excitons and phonons. This means the excitons are strongly coupled to just a few vibrational modes. As an alternative interpretation, its inverse can be taken, giving units of time:  $\tau_c = \frac{1}{\gamma}$ , where  $\tau_c$  is the characteristic time scale of energy fluctuations after excitation (aka, auto-correlation lifetimes).
- $\omega_0$  describes the location of the ”center“ of the peak, or the vibrational mode where electron-phonon coupling is the strongest.

In the HEOM derivation,  $\mathcal{J}(\omega)$  is our approximation for the imaginary part of the spectral response function, often denoted as  $\chi''(\omega)$ .

It is also important to note that for our systems, the spectrum of electron-phonon coupling is not continuous, and the plot of the spectrum will show “spikes” of coupling at each vibrational mode. We use the Drude-Lorentz model to approximate the spectral density as continuous. This document will provide an overview of the different parameters in the HEOM model and how varying these parameters affects coherent exciton lifetimes within a system. In addition to the above parameters, we will also investigate the electronic coupling between sites, denoted as  $J$ .

### 3.2 Spectral Density Parameters

#### 3.2.1 Varying $\lambda$

As seen from the formulation of  $\mathcal{J}(\omega)$ ,  $\lambda$  is a parameter that scales the Drude-Lorentz peak linearly. To test the effect of various values of  $\lambda$ , the GPU HEOM program was used. A two-site system was tested, and the values of  $\gamma$  and  $\omega_0$  were held constant (at 50 and 85 cm<sup>-1</sup>, respectively). The electronic Hamiltonian used is of the form  $(\begin{smallmatrix} \epsilon_0 & J \\ J & \epsilon_1 \end{smallmatrix})$ , where  $\epsilon$  is the site energy and  $J$  is the intersite electronic coupling. Values used here are:  $(\begin{smallmatrix} 100 & 50 \\ 50 & 0 \end{smallmatrix})$ . The resulting spectral densities and coherence plots are shown below:

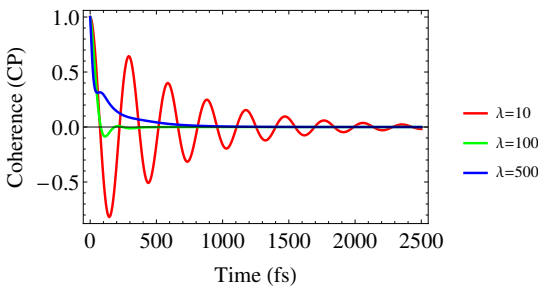


Figure 6: Coherence Lifetimes for various  $\lambda$

As can be seen, lower values of  $\lambda$  are associated with markedly longer coherence lifetimes. Figure 6, the plot of coherence lifetimes, plots an off-diagonal value of the density matrix  $\rho$ .  $\rho$  is a 2x2 matrix, where the diagonal elements are the populations of sites 1 and 2, and the off-diagonal elements describe the amount of coherence in the system.

So we can conclude that in general, lower reorganization energies lead to longer coherence lifetimes. If the reorganization energy is larger, the normal modes in the molecule are displaced more, more energy is lost to the environment after excitation, and the exciton localizes faster.

### 3.2.2 Varying $\gamma$

While investigating the effects of various values of  $\gamma$ , the same electronic Hamiltonian,  $(\begin{smallmatrix} 100 & 50 \\ 50 & 0 \end{smallmatrix})$ , was used.  $\lambda$  was set to 10 for all tests. When  $\omega_0$  was set to  $20 \text{ cm}^{-1}$ , the following results were seen for coherence lifetimes (with corresponding spectral densities on the right):

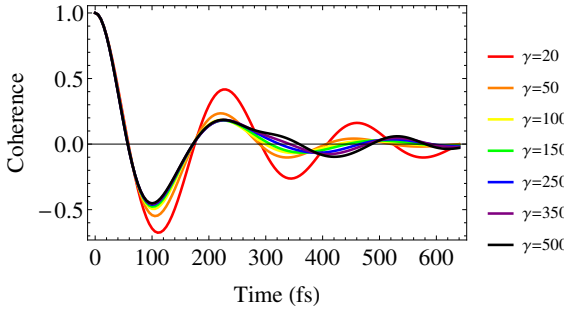


Figure 8: Coherence Lifetimes for various  $\gamma$  and a low peak center

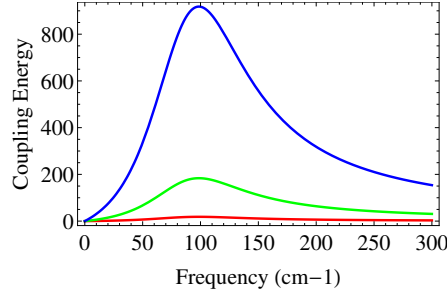


Figure 7: Drude-Lorentz spectral densities for various  $\lambda$

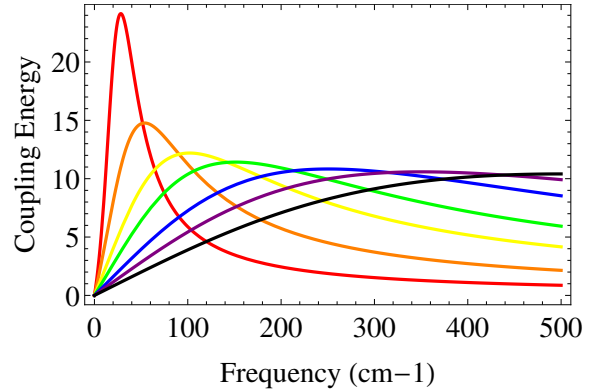


Figure 9: Drude-Lorentz spectral densities for various  $\gamma$  and a low peak center

So it appears that for spectral densities centered at low frequencies, a lower  $\gamma$  with all else held constant results in longer-lasting coherence.

To test if shifting the whole distribution to higher frequencies would have an effect on coherence lifetime, I next varied  $\omega_0$  while holding all else constant.

### 3.2.3 Varying $\omega_0$

To test the effects of the placement of the peak center,  $\omega_0$  (which is to say, testing the effects of coupling to certain frequencies), the same electronic Hamiltonian as previous trials was used. Additionally, the reorganization energy was set to 10 and  $\gamma$  was set to  $10 \text{ cm}^{-1}$ , with special attention paid to keeping  $\gamma$  low so as to generate a narrow spectral density peak and only have electron-phonon coupling to specific frequencies.

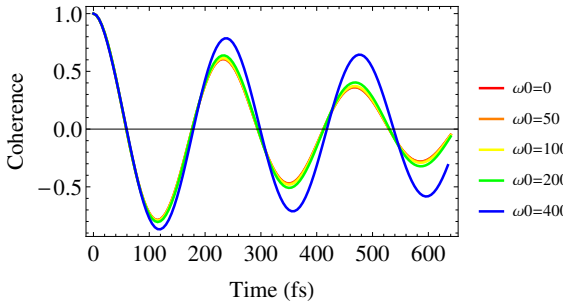


Figure 10: Coherence Lifetimes for various  $\omega_0$

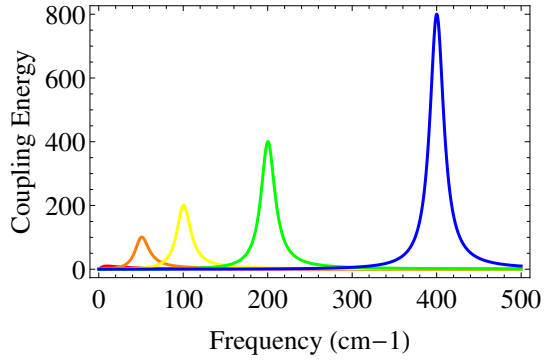


Figure 11: Drude-Lorentz spectral densities for various  $\omega_0$

As we can see, increasing  $\omega_0$  while holding all other parameters constant lead to increased coherence lifetimes at relatively high values of  $\omega_0$ , but there isn't a noticeable effect for values of  $\omega_0$  below  $200 \text{ cm}^{-1}$ .

The results thus far seem to indicate that to maximize coherent lifetimes, we want a system with a low reorganization energy  $\lambda$ , a low value of  $\gamma$  (coupling to narrow bands of vibrational frequencies), and coupling to high-frequency vibrational modes.

### 3.2.4 Side Notes

One potential question, especially when looking at Figure 11, is about whether we are truly isolating the different parameters. In Figure 11, we see that by increasing the  $\omega_0$  parameter in the denominator of  $\mathcal{J}(\omega)$ , we cause the peak to increase in height at higher values of  $\omega_0$ . Similar scaling issues seem to occur for other parameters - for instance, increasing  $\gamma$  makes the peak shorter. Should these scaling issues be eliminated by the introduction of new scaling parameters to maintain peak height no matter the value of  $\gamma$  or  $\omega_0$ ?

To see why scaling is not necessary, we look to a useful relation defining  $\lambda$ . In Kreisbeck's dissertation [6], he shows that the spectral density is related to the reorganization energy as follows:

$$\int_{-\infty}^{\infty} d\omega \frac{\mathcal{J}(\omega)}{2\omega\pi} = \lambda \quad (2)$$

This was the measure used to make sure that when fitting multiple peaks to a dataset, each peak configuration had the same reorganization energy. Scaling the peaks of a Drude-Lorentz fit would change the overall reorganization energy, and therefore should not be done in our original qualitative analysis of parameter behavior.

### 3.2.5 Experimenting with Fitting Multiple Peaks

When we are fitting multiple peaks to a dataset (taken from DFT software), we have multiple discretized peaks, each with their own associated reorganization energy. For example, if a system generates the following discrete spectral density, the question we want to answer is, how carefully do we need to fit our Drude-Lorentz spectral density to the data? Can we group several nearby peaks into one peak?

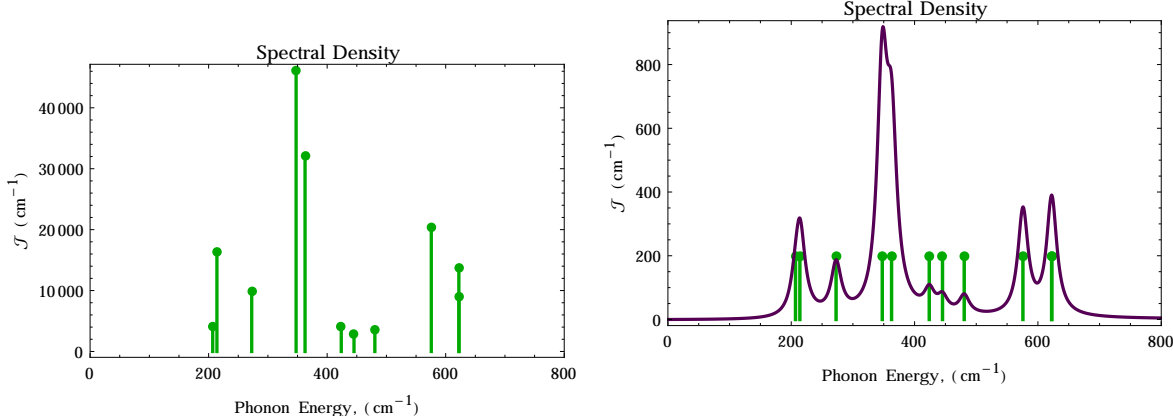


Figure 12: Discrete Spectral Density From DFT Software

Figure 13: Spectral Density with Drude-Lorentz fit (green peaks set to uniform height to show position)

In this case, each Drude-Lorentz peak was scaled by dividing its “actual” reorganization energy (from DFT) by its “calculated” reorganization energy (from the integration in Equation 2), thus avoiding the inaccuracy pointed out in the previous section.

To check the sensitivity of our system to the accuracy of fit, I compared the coherence lifetimes generated by a spectral density with two peaks, as opposed to one with a spectral density of one peak which overlaid the two peaks. The same electronic Hamiltonian was used as in the previous tests. The width of each smaller peak was set to  $30\text{ cm}^{-1}$ , and the peaks were centered at  $100$  and  $200\text{ cm}^{-1}$ . The reorganization energies of each peak were set fairly low and scaled so that they were roughly the same height, so one peak had  $\lambda=10$  and the other  $\lambda=5$ . Using these (somewhat arbitrary) values, the integration in Equation 2 was performed on the sum of these two Drude-Lorentz functions, and one larger peak was constructed with the resulting reorganization energy ( $\lambda=15$ ). This single larger peak was centered exactly between the two smaller peaks, and the width of the larger peak was varied. Values of  $\gamma=40$ ,  $\gamma=80$ , and  $\gamma=150$  were used, producing the following spectral densities and resulting coherence lifetimes:

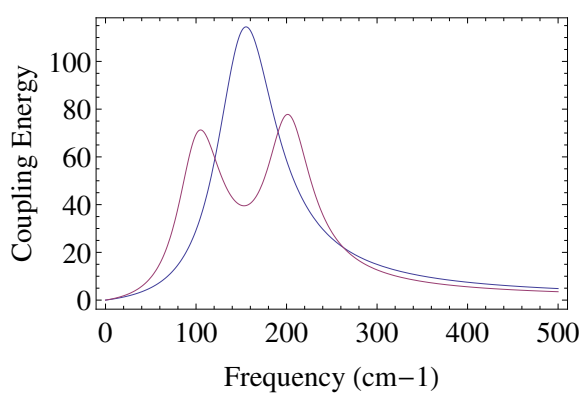


Figure 14: Superimposed peak with  $\gamma=40$

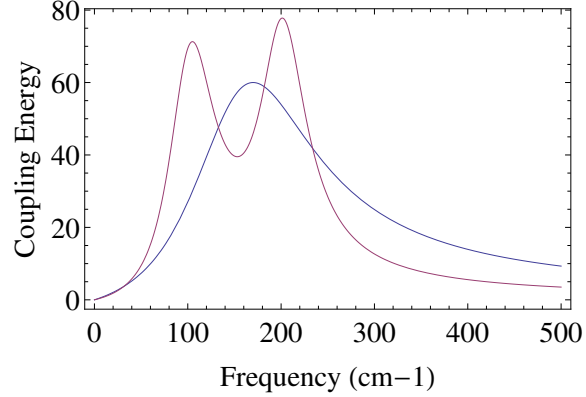


Figure 15: Superimposed peak with  $\gamma=80$

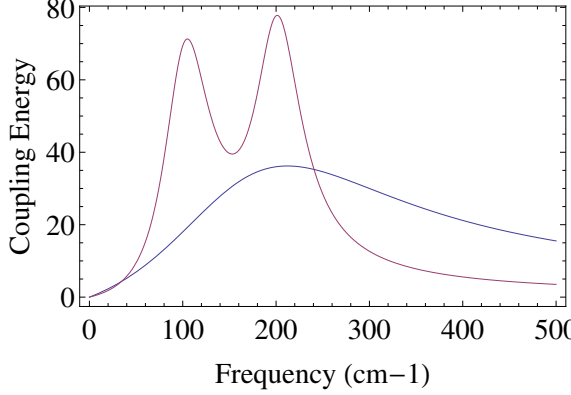


Figure 16: Superimposed peak with  $\gamma=150$

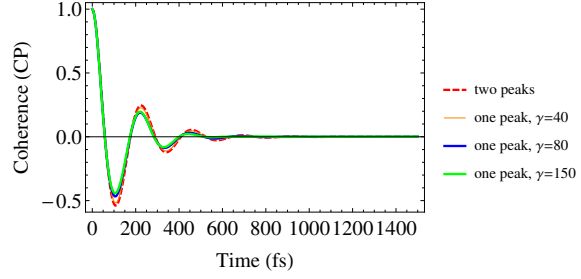


Figure 17: Resulting coherence lifetimes for three different fits

As can be seen in Figure 17, the differences in coherence lifetime are present but not terribly significant. As expected, coherence lifetime decreases slightly with increased  $\gamma$ , but behavior is nearly identical between the case with two peaks versus the case using one, more generalized, peak.

As the two smaller peaks are moved closer together, and their appearance approaches that of a single peak, the fit quality begins to have a larger effect. However, the overall behavior of the system is almost unchanged, even with qualitatively terrible fits, as long as  $\lambda$  is the same between the two spectral densities and the center of the larger peak aligns with the center between the two smaller peaks. The Drude-Lorentz approximation in the Heirarchical Equations of Motion is resilient to variation in peak fit.

### 3.3 Varying Intersite Electronic Coupling

In previous sections, we've kept the same electronic Hamiltonian, of the form  $(\begin{smallmatrix} \epsilon_0 & J \\ J & \epsilon_1 \end{smallmatrix})$ . The  $J$  here refers to the strength of the coupling between sites, while the spectral density  $\mathcal{J}(\omega)$  refers to the strength of the electron-phonon coupling of the whole system. By changing the value of  $J$  in the Hamiltonian while keeping a constant spectral density, we can determine the effect of the intersite coupling on coherent transport. For a range of different reorganization energies, peak widths, and peak locations, increasing the intersite coupling was found to increase coherent lifetimes, as well as increase the rate of population transfer between sites.

For example, with a  $\Delta\epsilon$  of 100 between sites,  $\lambda = 15$ ,  $\gamma = 10$ , and  $\omega_0 = 100$ , the following population behaviors were observed (where the red lines correspond to the exciton population at site 1, and the blue to site 2):

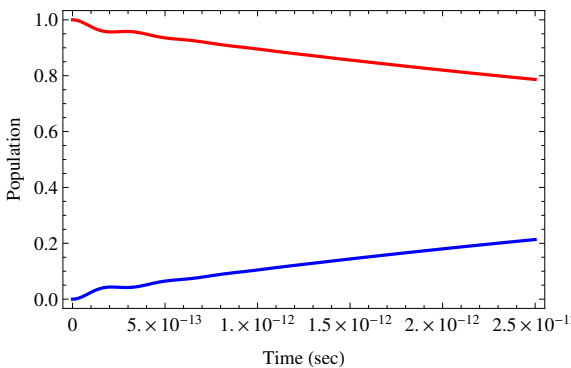


Figure 18: Population dynamics for  $J=10$

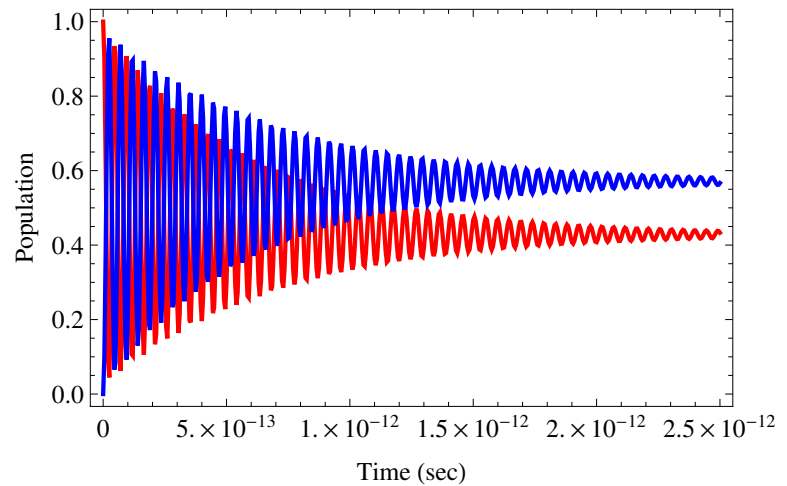


Figure 19: Population dynamics for  $J=350$

The difference in an order of magnitude in the intersite coupling was the difference between non-coherent and coherent behavior for this particular system. In addition, increasing J increases the rate at which energy moves between the two sites.

### 3.4 Conclusion of Parameter Analysis

After this analysis, we have observed several conditions which maximize coherent transport in a two-site system:

- Low reorganization energy
- Low  $\gamma$  (narrow coupling to phonon modes)
- High  $\omega_0$  (maximize coupling at higher vibrational frequencies)
- High intersite coupling, J (on the same order of magnitude or greater than spectral density peak position  $\omega_0$ )
- If multiple peaks exist in the discrete spectral density, a more accurate fit will produce a better model, but the most important parts of the fit are:
  - normalizing the Drude-Lorentz fits to have the correct reorganization energies, by integrating  $\frac{\mathcal{J}(\omega)}{\omega}$
  - making sure the Drude-Lorentz fit peaks are centered at the correct  $\omega_0$

The next step in our investigation was to use Density Functional Theory software to model and analyze the characteristics of real-world molecular systems.

## 4 DFT

### 4.1 Overview

In order to use the HEOM equations to model the real-world DN2, DN4, and DN6 systems, the electronic structure and vibrational nature of the constituent atoms of the system needed to be analyzed using Density Functional Theory (DFT). DFT is a computationally intensive method of modeling the electron density of many-bodied systems by solving the many-electron, time-independent Schrodinger equation [7]:

$$\hat{H}\Psi = [\hat{T} + \hat{V} + \hat{U}]\Psi = [\sum_i^n (-\frac{\hbar^2}{2m_i} \nabla^2) + \sum_i^n V(\vec{r}_i) + \sum_{i < j}^n U(\vec{r}_i, \vec{r}_j)]\Psi = E\Psi \quad (3)$$

The DFT software Q-Chem [9] was used extensively to acquire the pertinent data which was then analyzed and used to run the HEOM simulations. Supplying the HEOM with the necessary parameters taken from DFT analysis allowed us to arrive at the exciton transport dynamics within our molecular systems, namely the time scales during which coherent transport is maintained by DN2, DN4, DN6.

In order to simulate exciton dynamics, three important characteristics of the system needed to be calculated from the DFT data: the reorganization energy of the molecular sites, the exciton coupling between the two sites, and the spectrally resolved reorganization energy of the entire system. These characteristics, described in detail in the following subsections, are procured via geometry optimizations, electronic excitations, and Hessian (vibrational) analysis of the sites and full systems.

### 4.2 Reorganization Energy

As mentioned in Section 3, the reorganization energy of the sites in the system plays a major role in extending the coherence lifetime of an exciton within our system. Identifying molecules with low reorganization energies to be used as the site molecules is key to maintaining a long coherence lifetime. But what is reorganization energy, and how is it calculated by Q-Chem?

By solving the many-electron TISE (Equation 3), Q-Chem is able to optimize the geometry of a molecule by minimizing the energy of all of the atoms within a system according to a prescribed electronic configuration of the system. These electronic states can range anywhere from the ground state (all electrons are in their lowest occupiable orbitals) to any number of excited states (when an electron gains energy and occupies an orbital with an energy higher than the ground state orbitals) [9]. The reorganization energy of a molecule refers to the difference in energy between the un-optimized geometry of the molecule after excitation from the ground state, and the optimized geometry of the molecule in its first excited state. This energy difference is shown graphically in Figure 20.

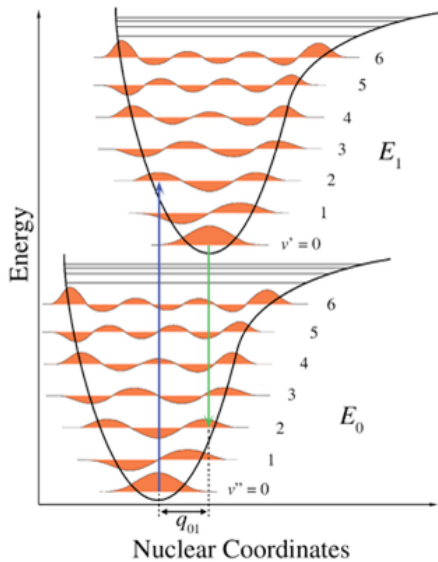


Figure 20: Reorganization Energy

The energy difference between the two states arises from the change in nuclear coordinates of the atoms during an excitation process. In Figure 20, a molecule is initially in its ground state and geometrically optimized. Upon excitation into its excited state, the atoms of the molecule will reorganize to achieve geometric optimization in the molecule's first electronic excited state. This movement of the atoms lowers the molecule's energy from when it was first excited, and this lowering of energy is referred to as the reorganization energy. Energy is transferred from the excitation of the electron into the physical geometry and phonon modes of the system - this is what causes electron-phonon coupling.

The reorganization energy of naphthalene was known to be low from previous calculations by Dr. Mark Lusk and Dr. Huashan Li, so it became the original choice of molecule to be used as the sites within our systems. Reorganization energy calculations on oligocenes (chains of benzene atoms) longer than naphthalene using Q-Chem were also conducted. Findings shown in Figure 21 indicate that longer chains of benzene molecules lead to lower reorganization energies. Therefore, in order to increase the coherence lifetime of an exciton within the system, longer chains of benzenes would need to be used as the site molecules in the system.

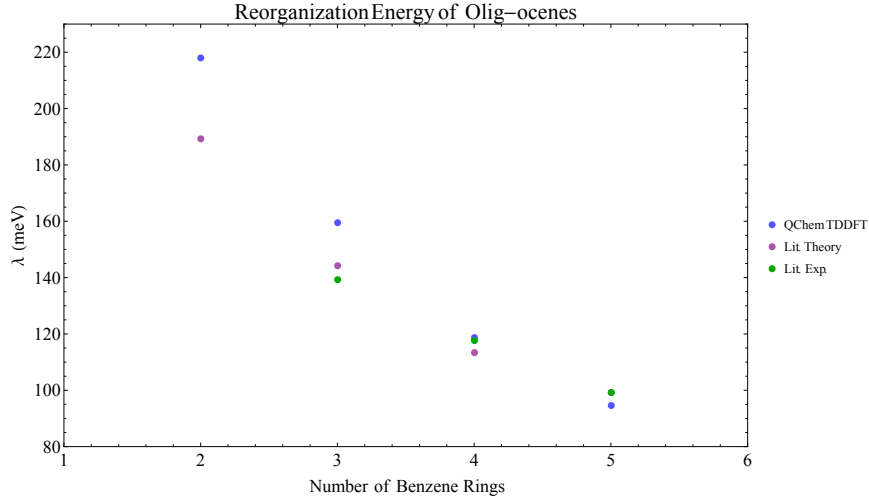


Figure 21: Reorganization Energies of Oligocenes

### 4.3 Vibrational Analysis

As mentioned in the overview, as the exciton moves throughout the system, the system's phonon modes couple with the exciton [7], causing it to decohere. Because of this, an analysis of the phonon modes within the system is necessary in order to be able to determine the exciton's transport dynamics. A Hessian (vibrational) analysis of the system using Q-Chem identifies the number of phonon (vibrational) modes of the system, the frequency of each vibrational mode, and the eigenvectors corresponding to the movement of each atom in association with each available vibrational mode within the system [9]. In short, the vibrational analysis determines the motion available to each atom within the system due to the available phonon modes of the system. Through a series of calculations, we spectrally resolved the reorganization energy, meaning we determined which phonon modes most strongly couple to the exciton. The spectral density described at length in Section 3 is directly fitted to this spectrally resolved reorganization energy using a Drude-Lorentz curve.

To arrive at the spectrally resolved reorganization energy, four Q-Chem calculations were run on the full systems:

- Geometry optimization of the full system in its electronic ground state
- Excitation of one naphthalene site and optimization of the naphthalene in its electronic first excited state
- Geometry optimization of the full system again, this time with one of its sites in an electrically excited state (via exciton creation)
- Vibrational analysis of the full system

The geometry optimizations calculate the displacement of the system's atoms as a result of excitation of one site and the subsequent relaxation of the whole system. A derivation of the spectrally resolved reorganization energy follows here [7].

Weighted by the square root of the mass of each atom  $n$ , each atom's "mass-weighted displacement" is calculated by:

$$\tilde{R}_n = (R_{1,n} - R_{0,n})\sqrt{m_n} \quad (4)$$

The vibrational analysis determines the eigenvectors that describe the movement of each atom in the system due to exciton-phonon coupling. A vector of the form

$$\vec{v}_n = (x_{1,n}, y_{1,n}, z_{1,n}, x_{2,n}, y_{2,n}, z_{2,n}, \dots, x_{m,n}, y_{m,n}, z_{m,n}) \quad (5)$$

describes the 3-dimensional eigencomponents of each atom  $n$  for every vibrational mode  $m$ .

The unitary matrix  $U$  is a matrix composed of all of the total eigenvectors of each atom and is defined as:

$$[U] = [\vec{v}_1, \vec{v}_2, \vec{v}_3, \dots, \vec{v}_n] \quad (6)$$

The amplitude of each eigenmode is given by

$$Q_m = [U] \cdot \tilde{R}_n \quad (7)$$

and the spectrally resolved reorganization energy for each vibrational mode  $m$  is given by

$$\lambda_m = \frac{1}{2} \omega_m Q_m^2 \quad (8)$$

where  $\omega_m$  is the frequency of the phonon mode.

Generating the spectrally resolved reorganization energy allows for a fitted Drude-Lorentz spectral density to be inserted into the HEOM. An example of our calculated data for a Naphthalene molecule is shown in Figure 22.

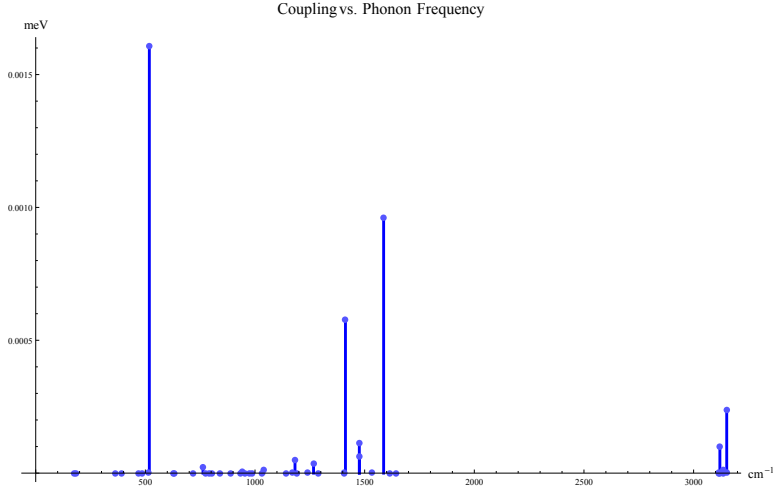


Figure 22: Spectrally resolved reorganization energy of Naphthalene

#### 4.4 Exciton Coupling

In Section 3.3 it was noted that by increasing the coupling between the sites of the system, the coherence lifetime of the exciton increases as does the energy transport between sites. Since decreasing the reorganization energy of the sites also increases coherence lifetime, an ideal system would increase the coupling between the sites while decreasing the reorganization energies of the sites themselves. Q-Chem FED (exciton coupling) calculations on the DN2, DN4, and DN6 systems indicate that increasing the length of the bridge decreases the coupling between sites [10]. Therefore, in terms of exciton coupling, the DN2 system is more ideally suited than DN4 and DN6 for maintaining exciton coherence for longer periods of time.

### 5 Overcoming Anderson Localization

The investigations performed into DN2, DN4, and DN6 systems suggested to us that it would be valuable to construct a chain of sites, in order to model energy transport more accurately. All previous analysis was done on two-site systems, but the HEOM is not limited to any number of sites except by computational limits.

One potential obstacle to energy transport down a chain of sites is Anderson localization. In the case where there is no electron-phonon coupling involved, Anderson calculated that in a perfectly ordered, homogenous system, electrons will not localize. However, if any disorder (in this case, in the form of differences in the site energies) is introduced, the electron will localize at the disordered site [11].

In our system, if we are hoping to construct a chain of molecules to transport excitons, there is no way to ensure that all sites will be exactly identical. Disorder is inherent to physical systems. The question is, is there a way to engineer molecules so that Anderson localization can be mitigated? Using electron-phonon coupling, energy can transfer between the electronic and phonon parts of the system and preserve coherence for longer than a system with no electron-phonon coupling.

To prove this, a system of nine sites was analyzed. Extreme disorder was introduced into the system: the site energies were (in  $\text{cm}^{-1}$ ): 939.0, 403.0, 1259.0, 1182.0, 586.0, 1864.0, 1057.0, 1928.0, 915.0. The electronic coupling between each site was  $100 \text{ cm}^{-1}$ . The spectral density was one peak, centered at 0, with a constant  $\gamma = 30$  and a variable reorganization energy. The results are shown in Figure 23:

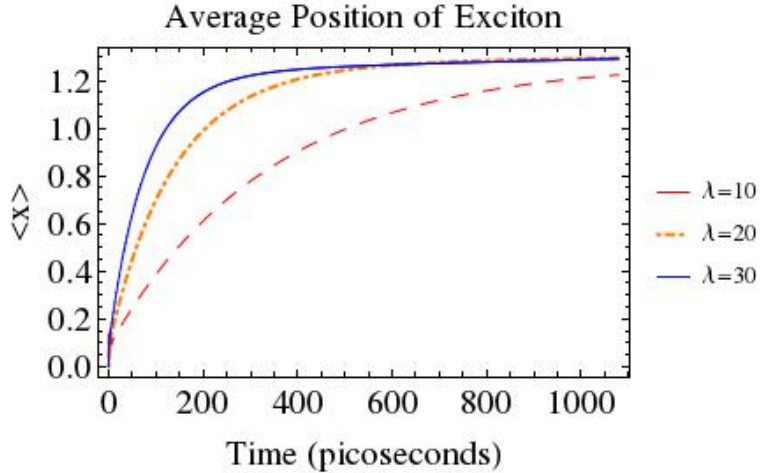


Figure 23: The effect of increasing reorganization energy on a system with large disorder.

As can be seen, for a system with very large disorder, increasing the reorganization energy causes the exciton to move further down the chain in the same amount of time. The case where  $\lambda = 0$  would correspond to Anderson localization, where the exciton population would localize very quickly. However, electron-phonon coupling overcomes this localization, increases transport rates, and is a very promising way to engineer coherence even in systems with unavoidable disorder.

## 6 Conclusion

Overall, this project has been successful in analyzing different molecular systems, understanding and implementing the Heirarchical Equations of Motion, and in expanding investigations into systems larger than two sites. The theory behind the HEOM derivation, such as Fluctuation Dissipation Theory, has been studied in depth. A detailed parameter analysis of the HEOM model has been performed to determine both the computational limits of the HEOM and to determine the ideal parameters for a coherent system. Density Functional Theory software has been used successfully to model systems and extract relevant information, such as spectrally resolved reorganization energy and electronic coupling. We have determined that longer bridges between two sites decreases electronic coupling, which inhibits coherence, but longer chains of carbon rings have lower reorganization energy, so a balance must be struck to maximize coherent transport. The ideal system for coherent transport has low reorganization energy, narrow modal bands of electron-phonon coupling, and high-frequency coupling. Using these conclusions, we have expanded our investigation to longer chains of sites, and we have discovered that including electron-phonon coupling in our model has overcome the obstacle of Anderson localization.

## 6.1 Future Work

Work by Ahsan Nazir suggests the potential impact of including correlations of phonon mode fluctuation between sites. Nazir analyzes a system with correlations included and no reorganization energy (the Redfield limit). Correlation is included with an ad hoc exciton-phonon coupling Hamiltonian,

$$\mathcal{H}_{ex-ph} = \sum_{j=1,2} |X>_j < X| \sum_k (g_k^j b_k^\dagger + g_k^{j*} b_k)$$

The  $g_k$  terms account for correlation. Nazir found that in the limit of complete fluctuation correlation, the system behavior is always coherent regardless of temperature [12].

This result shows that further consideration of vibrational correlations between sites is called for. To include correlations in the HEOM means to rederive (2), in terms of the response function and symmetrized correlation function of two-time correlation functions that may include correlation between sites. While such a derivation is out of the scope of this project, a method for considering vibrational correlations in molecular systems has been developed. See Appendix A for a general overview of the developed method for a simple system.

## A Vibrational Correlation Between Molecular Sites

In the current HEOM approach, an exciton is coupled with the phonon states of an electronic site. Electronic coupling between sites allows an exciton to move between sites. Physically, this coupling is related to overlapping orbitals. These orbitals, in turn, influence nuclear motion. In this way electronic coupling implies a degree of vibrational coupling. However, the current approach does not consider the "overlap" between phonon states of coupled electronic sites.

Coming from the point of view of delaying dissipative actions (both quatum "dissipation", decoherence, and energetic dissipation), the current models omission of an entire energetic pathway makes obvious a potential path for extending exciton coherence. The reorganization process is the only mechanism to consider the dynamics of a non-equilibrium phonon state. However, reorganization is a dissipative process ensuring decoherence. By considering how excitation can move through the phonon modes of each site, the coherent lifetime of the total system (exciton and phonon) stands to be increased.

In this appendix, a method for studying vibronic energy pathways between coupled sites for energy is developed. Coupled spring-mass systems are used to visual the method. Because the current formulation of the HEOM, when tracing out the phonon system, casts the bath expectation value as two-time correlation functions between phonon states, correlation between phonon modes was the desired metric to be calculated from the system. See Mathematica notebooks for many example routines. Below is an explanation of the routine used. A more clear and visual presentation can be found in kSchumacSnrDsnPoster.ppt.

In order to demonstrate how correlation between vibrational modes is conceived and calculated, consider a spring-mass system. Similar to the exciton transport detailed in 1.2, the full system will be composed of two subsystems and a bridge. In this case each "site" is a 3 mass 2 spring system, and the "bridge" is a mass with springs connecting to an edge of each site.

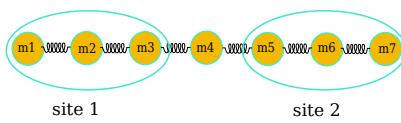


Figure 24: Example of a 2-Site System

First, a normal mode analysis is carried out for the substructures as well as the full structure; so that there are 3 sets of normal modes of various dimensions. Next, expand the substructure normal modes into the full structure basis; denote these expanded normal modes as  $\chi_{1,j}$  and  $\chi_{2,j}$  (note  $\chi_1$  and  $\chi_2$  are not normal modes of the full structure), where  $j$  indicates the mode and 1,2 indicate the site. This expansion must be done with some care. The masses (atoms in a molecular system) of the full structure (2 sites plus bridge) must be enumerated in such a way that the first bunch of indices refer to the first site masses, the second bunch of indices refer to the bridge, and the third bunch refer to the second site. Thus upon expansion into the full basis, the first site's normal modes will only have entries in the first bunch of indices, and the second site only in the second bunch of indices. If the bridge has no degrees of freedom then it is possible that the full structure has less DOFs than the sum of the two substructures. In this case there will be "spill over" in the expanded basis; normal modes from each site may have entries at the same index locations in the expanded basis.

After expanding the basis, a simulation of the full system dynamics is carried out. First, an initial condition,  $q(0)$ , is chosen (this corresponds to the initial phonon modes at the excitation site becoming excited due to their strong coupling with the exciton). Let the entire vibrational state of the system be denoted  $q(t)$ , where each entry in  $q(t)$  describes the motion of a certain mass. Next the overlap of  $q(t)$  into the normal modes of the substructures is calculated. This is achieved by performing an inner product between the normal mode and  $q(t)$ ; the result being a time series of the overlap, denoted  $\phi_{i,j}$  where  $i$  is the site and  $j$  is the normal mode.

$$\phi_{i,j}(t) = \langle \chi_{i,j} | q(t) \rangle$$

The correlation between normal modes at different sites can now be caculated as

$$\mathcal{C}_j(\tau)=\frac{\lim_{T\rightarrow \inf}\int\limits_0^{T_f/2}\phi_{1,j}(t)\phi_{2,j}(t+\tau)dt}{T_f}$$

## References

- [1] A. Ishizaki and G. Fleming, Unified treatment of quantum coherent and incoherent hopping dynamics in electronic energy transfer: Reduced hierarchy equation approach, *J. Chem. Phys.* 130, 234111 (2009); doi: 10.1063/1.3155372
- [2] C. Kreisbeck et al., "High-Performance Solution of Hierarchical Equations of Motion for Studying Energy Transfer in Light-Harvesting Complexes," *J. Chem. Theory Comput.* 2011, 7, 21662174; dx.doi.org/10.1021/ct200126d
- [3] A. Fisher, The Redfield Equation, <http://www.cmmp.ucl.ac.uk/~ajf/coursenotes/node42.html>. Accessed 30 September 2013.
- [4] The Franck-Condon Principle, [http://en.wikipedia.org/wiki/Franck-Condon\\_principle](http://en.wikipedia.org/wiki/Franck-Condon_principle). Accessed 30 September 2013.
- [5] A. Ishizaki and G. Fleming, Unified treatment of quantum coherent and incoherent hopping dynamics in electronic energy transfer: Reduced hierarchy equation approach, *J. Chem. Phys.* 130, 234111 (2009); doi: 10.1063/1.3155372
- [6] C. Kreisbeck, Quantum transport through complex networks from light-harvesting proteins to semiconductor devices, Dissertation (Universitt Regensburg, 2012).
- [7] V. May, O. Kuhn, "Charge and Energy Transfer Dynamics in Molecular Systems," 3rd edition, Wiley-VCH, March 2011.
- [8] J. Thijssen, "Computational Physics", 2nd edition, Cambridge, MA: Cambridge University Press, March 2007.
- [9] *Q-CHEM User's Guide*, Version 4.1, Q-Chem, Inc., Pittsburgh, PA, 2012.
- [10] C.P. Hsu, et al., "Characterization of the Short-Range Couplings in Excitation Energy Transfer", *J. Phys. Chem. C* 112, 1204 (2008).
- [11] D. Hundertmark, "A Short Introduction to Anderson Localization," University of Illinois Urbana-Champaign, September 2007.
- [12] Nazir, Ahsan. "Correlation-Dependent Coherent to Incoherent Transitions in Resonant Energy Transfer Dynamics." *Physical Review Letters*.
- [13] A. Klimkans, S. Larsson. "Reorganization energies in benzene, naphthalene, and anthracene", *Chemical Physics*, 189, 25 (1994).